Available online at www.sciencedirect.com
SCIENCE DIRECT®
International Journal of Solids and Structures 42 (2005) 21–36
INTERNATIONAL JOURNAL OF SOLIDS and STRUCTURES
www.elsevier.com/locate/ijsolstr

# Classification of compatibility paths of SDOF mechanisms

András Lengyel [a,*], Zsolt Gáspár [a,b]

[a] Department of Structural Mechanics, Budapest University of Technology and Economics, Muegyetem rkp. 3, H-1521 Budapest, Hungary
[b] Hungarian Academy of Sciences, Research Group for Computational Structural Mechanics, H-1521 Budapest, Hungary

Received 8 June 2004; received in revised form 6 July 2004
Available online 11 September 2004

**Abstract**

The compatibility paths of mechanisms with a single degree-of-freedom typically form sets of curves in the global representation space. We classify the different cases of compatibility by introducing an energy function. The result obtained also depends on which element of the mechanism is regarded as driven. The different singularity types are demonstrated by examples (split-vanish point, limit point, asymmetric bifurcation, infinitely degenerate bifurcation, hilltop point, compatibility surface).


*Keywords:* Mechanism; Compatibility path; Energy function; Singularity; Bifurcation; Classification

## 1. Introduction

A mechanism consisting of rigid bars with prescribed length and a given topology is called a mechanism with a single degree-of-freedom if it typically has compatible positions where applying a suitable displacement to a suitable element, the displacement of the other elements can be uniquely determined. Compatibility paths form a set of points which belong to compatible positions in the space of the state variables chosen to define the position of the mechanism. The compatibility paths usually consist of lines, which can intersect one another (bifurcation points).

Bifurcation points arise from special geometric configurations. If a mechanism is created with a special geometry, it may have certain positions where the number of instantaneous kinematic degrees-of-freedom increases. At these points the mechanism can change shape and continue its motion along a different path.

* Corresponding author. Tel.: +36 1 4634044; fax: +36 1 4631099.
*E-mail address:* andras_1@hotmail.com (A. Lengyel).

0020-7683/$ - see front matter © 2004 Elsevier Ltd. All rights reserved.
doi:10.1016/j.ijsolstr.2004.07.005

Bifurcations of compatibility paths have been studied by several researchers. Tarnai (1999) and Litvin (1980) have shown mechanisms producing asymmetric bifurcations. Lengyel and You (2003) discussed further examples and paralleled this phenomenon to the well-known equilibrium bifurcations of elastic structures. They made further examination with the aid of the elementary catastrophe theory (Lengyel and You, 2004). Their method was based on the analogy between equilibrium and compatibility equations.

The aim of this paper is to classify the points of the compatibility paths, especially bifurcation points. The classification utilizes, where possible, the classification system developed for the equilibrium paths of elastic structures with a single loading parameter. Knowing the equilibrium paths of the perfect structure, the approximate calculation of the diagram of the paths associated with small imperfections becomes considerably easier. The equilibrium analysis employs the total potential energy function of the structure. Similar functions can be formulated for mechanisms as well, such as the ones proposed by Tarnai (1990) or Géradin (2001).

In this paper we introduce an energy function, the minimum points of which define the points of the compatibility paths, and which helps to identify sections of the compatibility paths which can divide or disappear due to suitable imperfections. Such points have been called 'split-vanish' points by Lengyel (2002), which name we adopt here.

## 2. Choosing the state variables

The coordinates of all nodes of the structure uniquely determine the position of the structure, though other variables are usually used in order to minimize the number of state variables. It is to be mentioned that in many cases the displacement of an element can be uniquely defined by angles in larger intervals than by the Cartesian coordinates of a chosen point. One may think that one state variable is sufficient to describe the position of a SDOF mechanism, but unfortunately it is not always sufficient for the global description of the compatibility paths. The space of the variables required for a unique description is called global representation space (GRS) (Gáspár et al., 1997). If two compatibility paths intersect in this space, then it indeed belongs to a bifurcation point of the compatibility paths.

Fig. 1 shows three mechanisms with a single degree-of-freedom to demonstrate the required number of the state variables and a practical way of choosing them. Fig. 1a shows a single bar the position of which is uniquely given by angle $\alpha$. As all points in this one-dimensional space belong to compatible positions, such simple structures are not considered in the following.

In Fig. 1b angle $\alpha$ uniquely defines node A, the general position of which is associated with two different compatible positions of the other bar. Another datum (i.e. $y$) is required to distinguish between the two positions denoted by continuous and dashed lines, respectively.

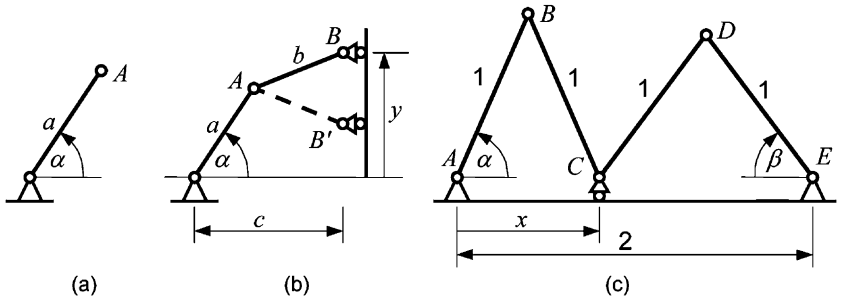


Fig. 1. SDOF mechanisms.

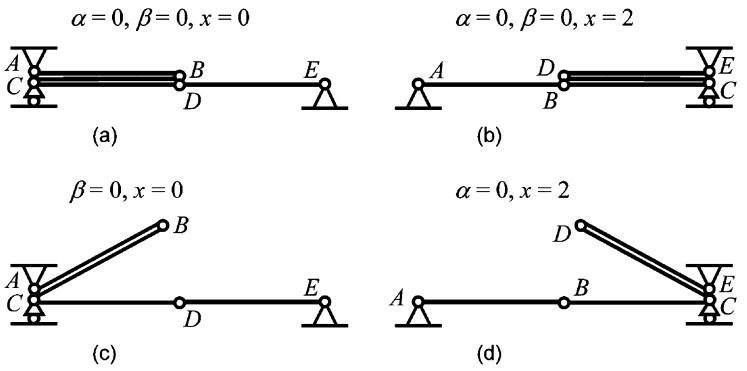


Fig. 2. Special positions of the four-bar linkage.

The structure shown in Fig. 1c consists of four bars of unit length, and the distance between the supports at the ends of the structure is 2 units. Now three state variables (i.e. $\alpha$, $\beta$ és $x$) are required for the global description of the compatibility paths of this structure. Fig. 2 demonstrates that though any position can be described by two variables, for any chosen two variables there can be found a position where the description is not unique. (Here and in the following bars covering each other are displayed with a small shift to make the picture clear.) Fig. 2a and b show that if the value of $\alpha$ and $\beta$ is set zero, two values can be found for $x$. If $\beta$ and $x$ are set as shown in Fig. 2c, $\alpha$ can be chosen arbitrarily. In a similar way, if $\alpha$ and $x$ are set as shown in Fig. 2d, $\beta$ can be chosen arbitrarily.

## 3. Compatibility equations

Though an appropriate choice of the state variables can uniquely define the positions of the nodes, conditions also need to be formulated to ensure the compatibility of the structure regarding bars the length of which has not been used to describe the nodes. In case of the structure shown in Fig. 1b, the length of bar AB needs to be prescribed, while in case of the other one shown in Fig. 1c, two conditions are required for bars BC and DE, one for each. The number of the equations is one less than that of the state variables. These conditions are called compatibility equations, and are formulated as

$$l_i(\phi_1, \ldots, \phi_{n+1}) - l_{i0} = 0, \quad i = 1, \ldots, n, \tag{1}$$

where the number of equations, the state variables, the distance of the corresponding nodes, and the prescribed bar lengths are denoted by $n$, $\phi_i$, $l_i$, $l_{i0}$, respectively. This non-linear equation system can usually be solved in a prescribed domain of the state variable space. For simple problems the curves can often be determined analytically while numerical methods may needed for complex ones. A numerical method is proposed in (Gáspár et al., 1997), which is able to find all solutions for the equation system $F = 0$ ($F$: $\mathbf{R}^{n+1} \rightarrow \mathbf{R}^n$) in a prescribed domain of the variable space.

## 4. Energy function

We introduce an energy function in terms of all state variables in order to classify the points of the compatibility paths:

$$V(\phi_1,\ldots,\phi_{n+1}) = \sum_{i=1}^{n} \frac{c_i}{2}\left[l_i(\phi_1,\ldots,\phi_{n+1}) - l_{i0}\right]^2. \tag{2}$$

If the constants $c_i$ are chosen appropriately, the function represents energy, in a similar way to strain energy of elastic structures, thus it is necessarily non-negative. In the compatible positions $V = 0$ holds, hence they are absolute minimum points of $V$. This statement is valid for arbitrary constants $c_i > 0$, therefore they are all set as unity for simplicity's sake in the following. In case of the structure shown in Fig. 1b, the energy function defined above is

$$V(\alpha, y) = \frac{1}{2}\left[\sqrt{(c - a\cos\alpha)^2 + (y - a\sin\alpha)^2} - b\right]^2, \tag{3}$$

which is shown in Fig. 3 as an example. The minimum points are highlighted by a thick line.

In the analysis of the equilibrium paths of elastic structures, the state variables are divided into a group of variables and a single load parameter. According to this, now one of the state variables $\phi_i$ is regarded as a parameter ($\lambda$) while the rest as variables ($\alpha_i$, $i = 1,\ldots,n$). Another reason for this separation can often be the need for the actuation of the mechanism by driving one of its elements. In this case the appropriate displacement component of the actuated element is regarded as parameter $\lambda$. A monotonous change of parameter $\lambda$ cannot control motion along compatibility paths which are in a plane perpendicular to the axis $\lambda$, moreover, the motion can get stuck when it reaches a point on a compatibility path, the tangent of which is in a plane perpendicular to the axis $\lambda$. Such points and sections are called critical regarding $\lambda$. If other state variables are chosen for the role of $\lambda$, other points of the compatibility paths can become critical. In order to track the entire compatibility set, at suitable points one may need to switch to another element to be actuated.

Thus the energy function (2) has not changed, only the state variables have been grouped into variables and a parameter (while $c_i$ are fixed):

$$V(\alpha_1,\ldots,\alpha_n;\lambda) = \sum_{i=1}^{n} \frac{1}{2}[l_i(\alpha_1,\ldots,\alpha_n;\lambda) - l_{i0}]^2. \tag{4}$$

In the points of the compatibility paths the equation system

$$\frac{\partial V}{\partial \alpha_i} = 0, \quad i = 1,\ldots,n \tag{5}$$

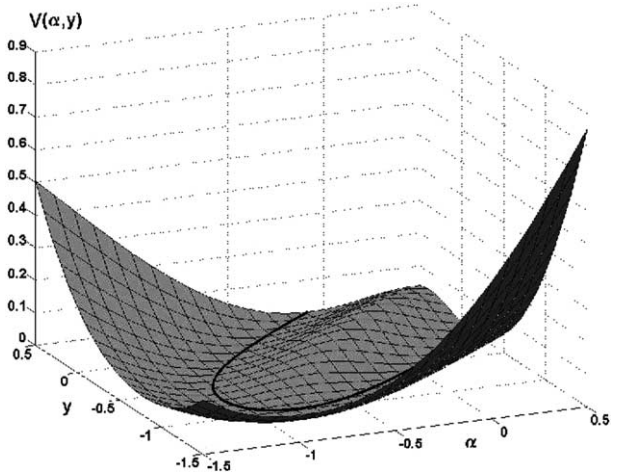


Fig. 3. Energy function.

holds, which can be formulated as

$$\begin{aligned}(l_1 - l_{10})\tfrac{\partial l_1}{\partial \alpha_1} + \ldots + (l_n - l_{n0})\tfrac{\partial l_n}{\partial \alpha_1} = 0,\\ \vdots\\ (l_1 - l_{10})\tfrac{\partial l_1}{\partial \alpha_n} + \ldots + (l_n - l_{n0})\tfrac{\partial l_n}{\partial \alpha_n} = 0.\end{aligned} \tag{6}$$

This is because at least one factor in each member becomes zero. The matrix form of the equation system is

$$\begin{bmatrix} \frac{\partial l_1}{\partial \alpha_1} & \cdots & \frac{\partial l_n}{\partial \alpha_1} \\ \vdots & \ddots & \vdots \\ \frac{\partial l_1}{\partial \alpha_n} & \cdots & \frac{\partial l_n}{\partial \alpha_n} \end{bmatrix} \begin{bmatrix} l_1 - l_{10} \\ \vdots \\ l_n - l_{n0} \end{bmatrix} = 0. \tag{7}$$

If the coefficient matrix becomes singular at a point, then the equation system (5) may hold even if the point is not a compatible position. At these points $V$ usually has local maxima or saddle points. It is to be mentioned that it occurs in other areas as well (i.e. thermodynamics) that only global minimum points of the energy function represent physically possible solutions (Poston and Stewart, 1978, Chapter 14).

If the coefficient matrix is not singular, then in case the equation is satisfied, all members of the vector are zero, the compatibility equations are satisfied, and $V$ has a (absolute) minimum. These are usually discrete points for fixed values of $\lambda$, and form compatibility paths when $\lambda$ is varying.

## 5. Classification of the points of the compatibility paths

The Hessian matrix of function $V$ is calculated in the points of the compatibility paths:

$$\mathbf{H}_V = \left[\frac{\partial^2 V}{\partial \alpha_i \partial \alpha_j}\right], \quad i,j = 1,\ldots,n. \tag{8}$$

If the Hessian is not singular (here it is positive definite), then the energy function is locally second-order. Such points are called regular points. If the Hessian is singular (here it is positive semidefinite, or maybe zero), then the point is critical.

The point is critical if it is either

- a limit point,
- a bifurcation point, or
- a split-vanish point.

The limit point is singular only regarding the chosen $\lambda$. If a different state variable is chosen for parameter, then the Hessian contains other derivatives of $V$ as well, and may not be singular. The compatibility paths often contain straight lines if the structure has special geometric dimensions. If a straight line is in a plane perpendicular to the axis $\lambda$, then all of its points are limit points forming a domain of continuum number of critical points. (Examples are shown for different types of critical points in Section 7).

At the bifurcation points two (or more) compatibility paths intersect. (Equilibrium paths may also produce a special case where the common point of the intersecting paths is their limit point at the same time. They are called hilltop points by Thompson and Hunt (1984).) In degenerate cases compatibility surfaces may be obtained in the bifurcation points. A similar singularity can be found for equilibrium paths, i.e., in

case of a compressed bar with a circular cross-section or in case of a structure under a following load shown by Gáspár and Mladenov (1995).

A critical point is called split-vanish point, if it is not a bifurcation point, not a limit point (at least $\lambda$ can be chosen so that it is not a limit point), though the Hessian matrix is singular. Sections (between two bifurcation points) consisting of such points can either split to two (or more) compatibility paths or disappear due to suitable imperfections.

## 6. Classification of bifurcation points

The bifurcation points of equilibrium paths are classified by the potential function of elastic structures in (Thompson and Hunt, 1984; Gáspár, 1999). The classification utilizes Thom's theorem (Poston and Stewart, 1978) known from the catastrophe theory, though due to the special role of the load parameter, different subclasses of certain catastrophe types have been distinguished.

The catastrophe points of the energy function introduced above cannot be directly used to classify the bifurcation points of the compatibility paths for three reasons.

- The energy function is special, for even the system with the allowed perturbations satisfies the condition $V \geqslant 0$.
- Not all stationary points of the energy function belong to compatibility paths, only the minimum points (only where $V = 0$ holds).
- It is an important point to distinguish between stable and unstable positions in the equilibrium paths. In case of the compatibility paths there is no such distinction, every compatible position is 'stable', hence the dual forms of the catastrophe types cannot occur.

In spite of this, we would like to utilize the experience obtained from the analysis of the bifurcation points of the equilibrium paths. The analysis of the equilibrium paths has not dealt with cases where some sections of the paths can split, hence here we intend only to classify bifurcation points which have no split-vanish compatibility paths. (A similar phenomenon has been found for equilibrium paths: Gáspár and Németh (2002) and Gáspár (2003) have shown a structure with a double cusp catastrophe point at which the paths could split. We also mention that Domokos (1991) has shown an elastic structure where the load parameter has a critical interval. The equilibrium path can bifurcate at all points of this interval, and moreover, the type of bifurcation may change within the section.)

So far we have dealt with bifurcation points where two compatibility paths intersect. In case of elastic structures, cuspoid catastrophe points always result in bifurcation points where two paths intersect. In the neighbourhood of the cuspoid catastrophes, the equilibrium paths can be well-displayed in the plane of the single active variable ($x$) and the load parameter ($\lambda$). The neighbourhood of the bifurcation point of the compatibility paths can be adequately described by two suitably chosen state variables, one of which is regarded as a parameter ($\lambda$), while the other as an active variable ($x$). If the shape of the compatibility paths is identical to that of the equilibrium paths of a catastrophe type, then the bifurcation point is regarded as of that certain type, in spite of the significant difference between the two energy functions.

Fig. 4 shows the equilibrium paths in the neighbourhood of the bifurcation point occurring for different cuspoid catastrophe types. The equilibrium paths of the so-called perfect structure are denoted by thick lines, and those obtained by a possible perturbation are denoted by thin lines.

The function of the secondary equilibrium paths shown in Fig. 4a–e are of the first, the second, the third, the fourth and the fifth order (omitting the constant member), respectively, and they may occur at the fold, the cusp, the swallowtail, the butterfly and the wigwam catastrophe points, respectively. This series can be extended arbitrarily. Arnol'd (1972) introduced the notation $\mathrm{A}_k$ ($k = 2, 3, \ldots$) for the cuspoid catastrophes.

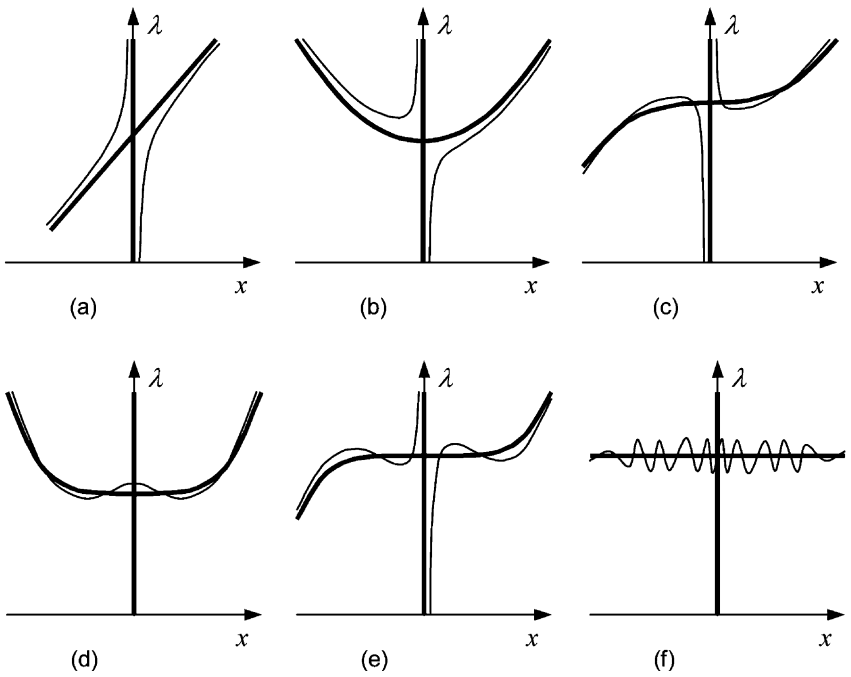


Fig. 4. Different types of bifurcations of equilibrium and compatibility paths.

The secondary equilibrium path shown in Fig. 4f is a straight line, which represents a case degenerate in infinite order. We mention that we do not show the equilibrium paths at stable and unstable symmetric bifurcation points separately because they are geometrically identical, difference can only be made regarding the stability of the equilibrium positions, while no such distinction applies to the compatibility paths.

Fig. 4 also shows the effect of imperfections which result in a $k$ number of equilibrium positions for a suitably chosen $\lambda$ in the neighbourhood of the bifurcation point. The index $k$ in Arnol'd's notation refers to the maximum number of stationary points, hence the number of equilibrium positions cannot be more than that. The type of a critical point of the equilibrium paths is defined by the order of the Taylor series expansion of the total potential energy function in terms of the active variable at the bifurcation point. Though the order of a similar Taylor series of the energy function introduced for compatibility paths is double that of the above function, the possible maximum of the number of minimum points of the energy function with a suitable perturbation is also $k$. Hence it is an acceptable proposition to classify the bifurcations of the two systems as of the same type based on the similarity of the neighbourhood of the bifurcation points.

If an actuated element of a mechanism has been designated, then the role of the parameter $\lambda$ is set in a similar way to equilibrium analysis, hence each bifurcation point can be associated with a unique classification. On the other hand, if none has been designated, then a bifurcation point may have different classifications depending on the choice.

## 7. Examples

### 7.1. Six-bar model

The global description of the compatibility paths of the mechanism shown in Fig. 5 (dashed lines also denote rigid bars) requires four state variables, which are also displayed in the figure. Bars AE and BF have

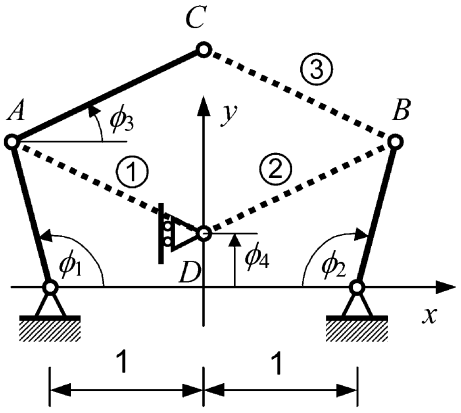


Fig. 5. The six-bar model.

unit length, the other four have $\sqrt{2}$, the fixed supports are at a unit distance from the origin, and node D can move only along axis $y$. The four state variables and the length of bars EA, FB, and AC uniquely determine the position of the nodes:

$$\begin{aligned}
&\mathrm{A}(-1+\cos\phi_1, \sin\phi_1),\\
&\mathrm{B}(1-\cos\phi_2, \sin\phi_2),\\
&\mathrm{C}\left(-1+\cos\phi_1+\sqrt{2}\cos\phi_3, \sin\phi_1+\sqrt{2}\sin\phi_3\right),\\
&\mathrm{D}(0,\phi_4).
\end{aligned} \tag{9}$$

To ensure the compatibility of the entire structure, one only needs to satisfy the compatibility equations for the three bars labelled with numbers:

$$\begin{aligned}
F_1 &= \sqrt{(x_\mathrm{A}-x_\mathrm{D})^2+(y_\mathrm{A}-y_\mathrm{D})^2}-\sqrt{2}=0,\\
F_2 &= \sqrt{(x_\mathrm{B}-x_\mathrm{D})^2+(y_\mathrm{B}-y_\mathrm{D})^2}-\sqrt{2}=0,\\
F_3 &= \sqrt{(x_\mathrm{B}-x_\mathrm{C})^2+(y_\mathrm{B}-y_\mathrm{C})^2}-\sqrt{2}=0.
\end{aligned} \tag{10}$$

The solution of these equations provides the compatibility paths, which lie in a four-dimensional space. Fig. 6 shows several characteristic positions of the mechanism that are labelled with numbers. The bars connected to node C are displayed in two possible positions in the figures, plotted by dashed and dotted lines, respectively. If the two positions do not coalesce, single and double quotes are added to the number, referring to the positions denoted by dashed and dotted lines, respectively. It is easy to figure out that the compatibility paths can bifurcate at positions 1, 2′, 2″, 3′, 3″, 5, 7′, 7″, 9, 11′, 11″ and 12.

Fig. 7 shows the two-dimensional projections of the compatibility paths. The numbered positions are also marked in the diagram. The set of compatibility paths consists of four closed loops and two straight lines. Curve A connects positions 1, 2′, 3′, 12, 11′, 7′ and 1, B connects 1, 2″, 3″, 12, 11″, 7″ and 1, C connects 5, 4″, 3″, 10″, 9, 8″, 7″, 6″ and 5, and finally, D connects 5, 4′, 3′, 10′, 9, 8′, 7′, 6′ and 5. One of the straight lines fits to points 2′ and 2″, while the other to 11′ and 11″.

The two straight lines are projected to a single point in figure $(\phi_1,\phi_2)$. The projections of two curves (C, D) coalesce, while the other two (A, B) not only coalesce but are seen as lines, too. In the projection $(\phi_2,\phi_3)$ the two straight lines cover each other, the wider loop represents the projection of three curves

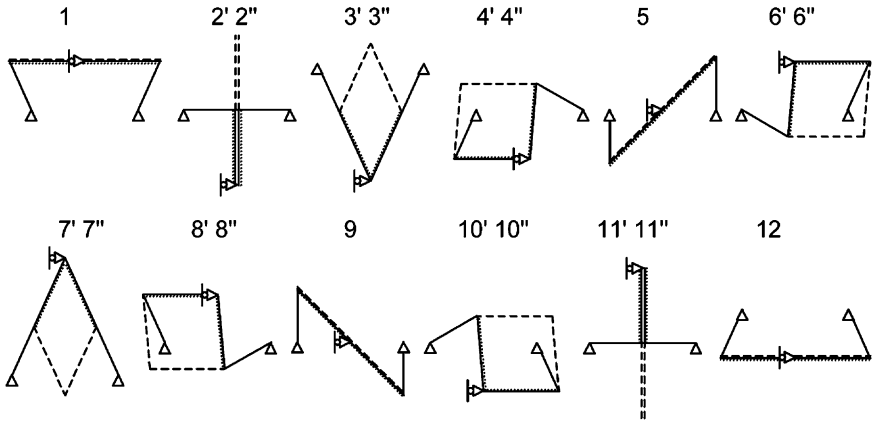


Fig. 6. Special positions of the six-bar model.

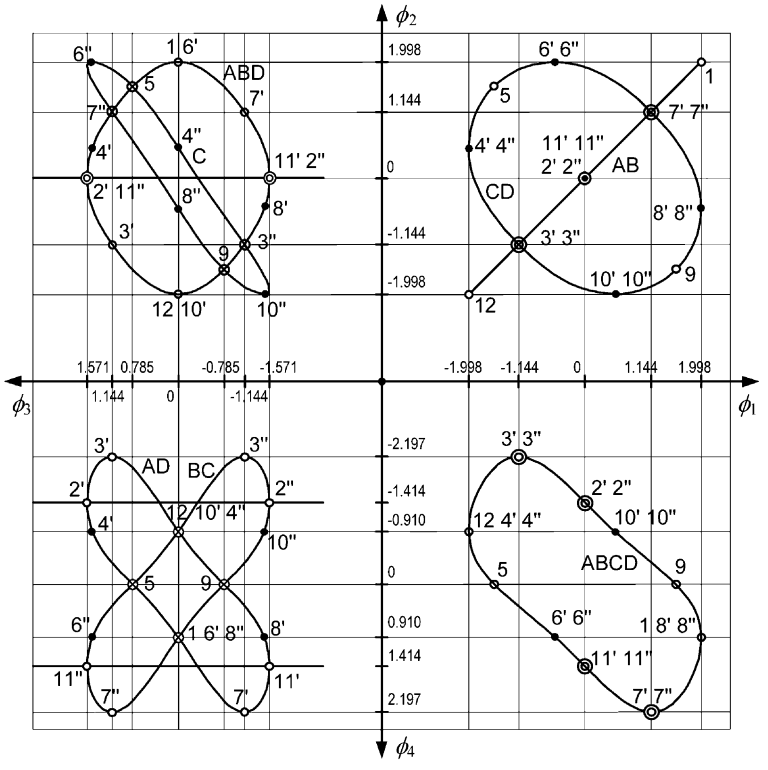


Fig. 7. Compatibility paths of the six-bar model.

(A, B, D), while the narrower one represents that of curve C only. On the coordinate plane ($\phi_3, \phi_4$) the two lines separate, and the projections of the curves coalesce in pairs. Finally, on the plane ($\phi_4, \phi_1$) the two lines are shown as points, and all four curves have the same projection.

At certain points the curves covering one another may intersect, while at other points the apparently crossing curves have no real intersection points. To visualize this, we introduce notations as follows. A blank circle and a double blank circle is used to denote a single bifurcation point and two bifurcation points covering each other, respectively. Four bifurcation points cover one another at the point $(0,0)$ on the plane $(\phi_1,\phi_2)$, which also represents the two straight lines entirely. This is denoted by a blank circle and a filled circle. Lines passing through circles refer to independent compatibility paths in addition to bifurcations. Crossing lines without mark refer to non-intersecting compatibility paths.

Three of the labelled points (4″, 7″, 2′) are analysed in detail, for which the energy function of the structure is formulated:

$$V = \frac{1}{2}F_1^2 + \frac{1}{2}F_2^2 + \frac{1}{2}F_3^2. \tag{11}$$

Point 4″ is given by its four coordinates:

$$(\phi_1,\phi_2,\phi_3,\phi_4) = (-1.9979, 0.5211, 0, -0.9102). \tag{12}$$

First let us choose $\phi_2$ as $\lambda$. Calculating the Hessian matrix using the derivatives with respect to $\phi_1$, $\phi_3$, and $\phi_4$, and evaluating it at the coordinates of point 4″ gives:

$$\mathbf{H}_{4''}^{1,3,4} = \frac{4}{9-4\sqrt{2}}\begin{bmatrix} 11\left(5\sqrt{2}-7\right) & 18-13\sqrt{2} & 0 \\ 18-13\sqrt{2} & 4\left(-1+\sqrt{2}\right) & 0 \\ 0 & 0 & 2\left(-1+\sqrt{2}\right) \end{bmatrix}, \tag{13}$$

whose rank is 3, hence the point is not critical and certainly not a split-vanish point. Fig. 8a shows the compatibility paths in the neighbourhood of the point projected to the plane $(\phi_1,\phi_2)$. If $\phi_1$ is chosen as $\lambda$, then the Hessian with respect to $\phi_2$, $\phi_3$, and $\phi_4$ yields

$$\mathbf{H}_{4''}^{2,3,4} = \frac{4}{9-4\sqrt{2}}\begin{bmatrix} -17+13\sqrt{2} & 6-5\sqrt{2} & 3\sqrt{2}-5 \\ 6-5\sqrt{2} & 4\left(-1+\sqrt{2}\right) & 0 \\ 3\sqrt{2}-5 & 0 & 2\left(-1+\sqrt{2}\right) \end{bmatrix}, \tag{14}$$

whose rank is 2, i.e., the point is critical. Fig. 8b shows that the compatibility path has a local limit point.

The coordinates of point 7″ are

$$(\phi_1,\phi_2,\phi_3,\phi_4) = (1.1437, 1.1437, 1.1437, 2.1974). \tag{15}$$

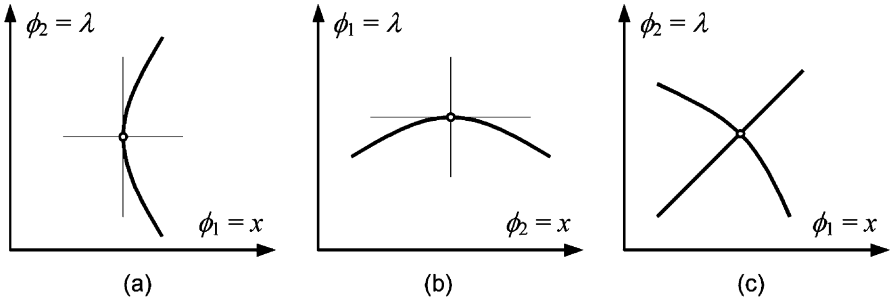


Fig. 8. Regular point (a), limit point (b), asymmetric point of bifurcation (c).

Let us choose $\phi_2$ as $\lambda$. At this point the Hessian with respect to $\phi_1$, $\phi_3$, and $\phi_4$ gives:

$$\mathbf{H}_{7''}^{1,3,4} = \begin{bmatrix} -56+40\sqrt{2} & 80-56\sqrt{2} & 0 \\ 80-56\sqrt{2} & -112+80\sqrt{2} & 0 \\ 0 & 0 & -4+4\sqrt{2} \end{bmatrix}, \tag{16}$$

whose rank is 2, i.e., point $7''$ is critical. Fig. 8c again shows the compatibility paths in the neighbourhood of the point projected to the plane $(\phi_1, \phi_2)$. (This figure can also be obtained by using only variables $\phi_1$ and $\phi_2$ for the description of the vicinity of the point. The larger one of the two possible values of $\phi_4$ is chosen, and only the compatibility equation for bar BC is to be satisfied. Node C is always in the topmost position.) This is an asymmetric point of bifurcation. Choose $\phi_4$ as $\lambda$ and calculate the Hessian with respect to $\phi_1$, $\phi_2$, and $\phi_3$:

$$\mathbf{H}_{7''}^{1,2,3} = \begin{bmatrix} -56+40\sqrt{2} & 0 & 80-56\sqrt{2} \\ 0 & 0 & 0 \\ 80-56\sqrt{2} & 0 & -112+80\sqrt{2} \end{bmatrix}. \tag{17}$$

The rank of this is 1, i.e., the decrement is 2, hence two active variables are required to describe the phenomenon, e.g., $\phi_1 = x$, $\phi_2 = y$. In the neighbourhood of the point, $\phi_3$ can always be chosen so that $F_3$ equals zero, leaving the other two equations only to deal with. The compatibility paths (Fig. 9) in the space $(x, y, \lambda)$ correspond to the well-known hilltop equilibrium path, which is a class of the hyperbolic umbilic catastrophe. We emphasize that this bifurcation can be regarded either as an asymmetric bifurcation or as a hilltop point, still the same perturbed compatibility paths must be obtained by introducing small imperfections. A similar statement applies to point $4''$, which was classified as critical or regular depending on the choice of $\lambda$. However, the perturbed compatibility paths are independent from this qualification.

The third point to examine is $2'$. The coordinates are

$$(\phi_1, \phi_2, \phi_3, \phi_4) = \left(0, 0, \pi/2, -\sqrt{2}\right). \tag{18}$$

Let us first check whether or not the connecting compatibility paths are split-vanish paths. The equation of the connecting straight line is

$$\left(\phi_1 = \phi_2 = 0, \phi_4 = -\sqrt{2}\right). \tag{19}$$

Let us choose $\phi_3$ as $\lambda$, and substituting the equation of the line into the Hessian matrix with respect to $\phi_1$, $\phi_2$, and $\phi_4$ gives:

$$\mathbf{H}_{2}^{1,2,4} = \begin{bmatrix} 2-\cos^2\phi_3 & -1+\cos^2\phi_3 & -1 \\ -1+\cos^2\phi_3 & 2-\cos^2\phi_3 & -1 \\ -1 & -1 & 2 \end{bmatrix}. \tag{20}$$

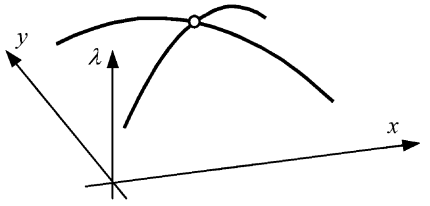


Fig. 9. Hilltop point.

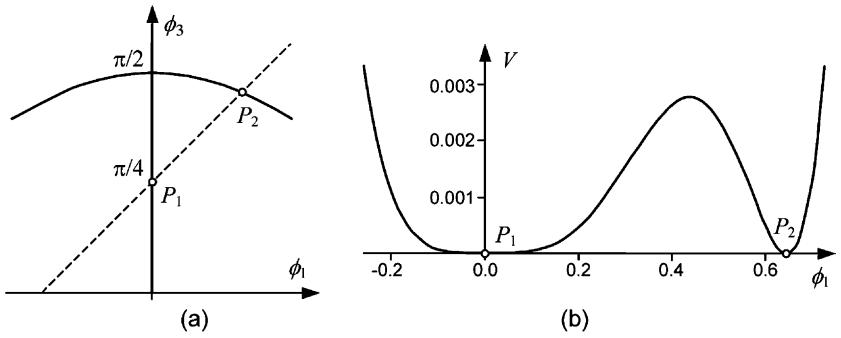


Fig. 10. Space of the state variables (a) and the energy function in a section denoted by the dashed line (b).

The rank of this is 2, hence all points of the straight line are critical. (We mention that the same result can be obtained regardless which state variable is chosen for $\lambda$.) Let us calculate a section of the potential function in order to determine the type of the critical points! Choose $\phi_2$ and $\phi_4$ in terms of $\phi_1$ so that the linkage EADBF is compatible, thus now the energy function of the structure consists of the member referring to bar BC only. Examine the cross-section $\phi_3 = \phi_1 + \pi/4$ (Fig. 10a). Fig. 10b shows the energy function in terms of $\phi_1$:

$$V(\phi_1) = \frac{1}{2}\left[\sqrt{4(1-\cos\phi_1)^2 - 4\sqrt{2}(1-\cos\phi_1)\cos(\phi_1+\pi/4)+2} - \sqrt{2}\right]^2. \tag{21}$$

The Taylor series expansion of the energy function (21) proves that the function is fourth order in point $P_1(\phi_1 = 0)$:

$$V_{P_1} = \frac{1}{4}\phi_1^4 - \phi_1^5 - \frac{1}{3}\phi_1^6 + \ldots \tag{22}$$

A similar expansion can be obtained if the cross-section is taken through any point of the straight line (19), i.e., the points of the line are split-vanish points.

To demonstrate the split-vanish paths, the perturbed compatibility paths are shown due to four different imperfections, which are introduced in Fig. 11a. If the supports are pulled apart to a small extent in a symmetric way to axis $y(\varepsilon_1 > 0)$, then the entire straight compatibility path disappears, while if they are pushed closer to each other ($\varepsilon_1 < 0$), it splits up. The two cases are denoted by thin dashed and continuous lines, respectively, in Fig. 11b in the neighbourhood of point $2'$ in the coordinate system $(\phi_1, \phi_3)$. The original

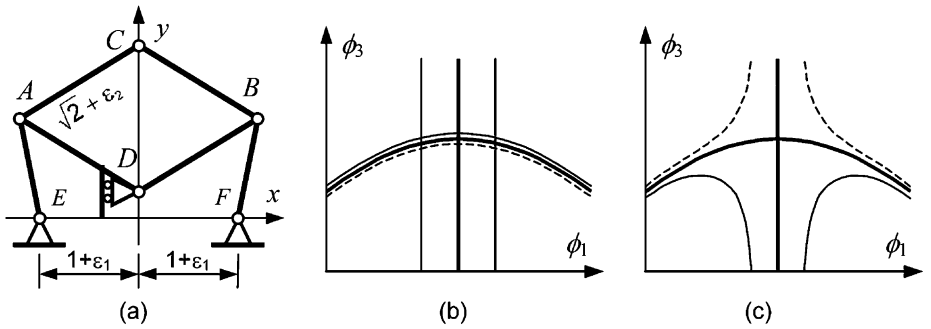


Fig. 11. Split-vanish compatibility path.

compatibility paths consist of a vertical straight line and a curve crossing it, as we have seen earlier. They have now changed to either a single thin dashed curve only or a double thin straight line and a curve crossing both. If the length of bar AC is perturbed ($\varepsilon_2 > 0$), then the section of the compatibility path between $2'$ and $2''$ splits up, while other sections disappear. In case of an imperfection of the opposite sign, the situation is the opposite, the section between $2'$ and $2''$ disappears and those outside of the original bifurcation points split up. The two cases are denoted by thin continuous and dashed lines, respectively, in Fig. 11c. (The compatibility paths of the perfect structure are plotted by thick continuous lines.)

### 7.2. The four-bar mechanism

Consider a structure consisting of three bars shown in Fig. 12a. The length of the bars and the distance between the supports are unity. In mechanical engineering this structure is considered a four-bar linkage as another bar is inserted between the supports forming a closed loop whose internal motions are examined. Hence in the following we use this name in accordance with mechanical engineering terminology.

Two state variables are required to describe the motion, $\phi_1$ and $\phi_2$, which determine the position of nodes A and B. The only compatibility condition refers to bar AB:

$$F = \sqrt{(1+\cos\phi_2-\cos\phi_1)^2+(\sin\phi_2-\sin\phi_1)^2}-1. \tag{23}$$

In the domain shown in Fig. 12b, the compatibility paths consist of three straight lines. The equations are

(a) $\phi_1 = \phi_2$,

(b) $\phi_2 = \pi$,

(c) $\phi_1 = 0$.

The energy function of the structure:

$$V = \frac{1}{2}F^2 = \frac{1}{2}\left(\sqrt{(1+\cos\phi_2-\cos\phi_1)^2+(\sin\phi_2-\sin\phi_1)^2}-1\right)^2. \tag{24}$$

Give qualifications for all three lines for both choices of $\lambda$! The Hessian matrices in the case of $\lambda = \phi_1$:

$$\mathbf{H}_a^2 = [\sin^2\lambda], \qquad \mathbf{H}_b^2 = [\sin^2\lambda], \qquad \mathbf{H}_c^2 = [0]. \tag{25}$$

All points of the lines (a) and (b) except $\lambda = k\pi$, $k \in \mathbf{Z}$ are regular, line (c) is entirely singular, i.e., infinitely degenerate (set of degenerate limit points).

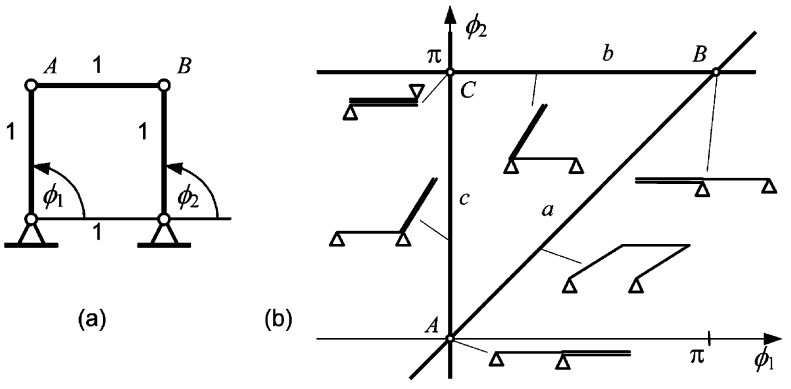


Fig. 12. The four bar linkage (a) and its compatibility paths (b).

If $\phi_2$ is chosen as $\lambda$:

$$\mathbf{H}_a^1 = [\sin^2\lambda], \qquad \mathbf{H}_b^1 = [0], \qquad \mathbf{H}_c^1 = [\sin^2\lambda]. \tag{26}$$

All points of the lines (a) and (c) except $\lambda = k\pi$, $k \in \mathbf{Z}$ are regular, line (b) is entirely singular, i.e., infinitely degenerate (set of degenerate limit points).

At the bifurcation points (where the Hessian with respect to both choices of the variables is singular), the order of the function of the secondary compatibility paths (Fig. 4) is summarized in the table below:

| Bifurcation point | $\lambda = \phi_1$ | $\lambda = \phi_2$ |
|---|---|---|
| A $(0,0)$ | Infinite | 1 |
| B $(\pi,\pi)$ | 1 | Infinite |
| C $(0,\pi)$ | Infinite | Infinite |

In order to determine these values, one needs to set the value of $\lambda$ at the bifurcation points, and expand the energy function into Taylor series in terms of the other variable up to the first non-zero member. In the first-order case (asymmetric bifurcation), the coefficient of the fourth-order member is not zero, and in the infinite-order case, the cross-section of the energy function is exactly the zero function.

If the order of the Taylor series is 4, then at most two compatible positions can be obtained in the neighbourhood of the bifurcation point at a fixed value of $\lambda$ due to a small perturbation of the system. In the infinitely degenerate case arbitrary number of compatible positions can be obtained due to suitable perturbations.

### 7.3. Spatial mechanism

Consider the spatial generalization of the six-bar mechanism introduced in Section 7.1 (Fig. 13a). The supports are placed on the perimeter of a unit circle at an equal distance from one another on the plane $(x,y)$. Point E is supported by a rail enabling it to move along axis $z$ only. This point is connected to the fix supports by three two-bar chains. Point D is connected to points A, B, and C by one bar each. The motion of these points is restricted to planes fitting to axis $z$ due to the planar joints at the supports. All other connections of the structure are spherical joints and all bars are of unit length.

Six state variables are required to describe the motion of the structure: three for the position of points A, B, and C, two for the relative position of D with reference to A, and one for the position of point E along $z$.

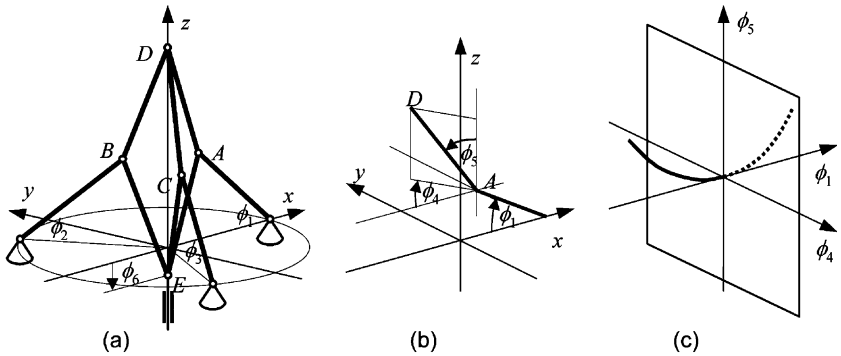


Fig. 13. Generalization of the six-bar linkage (a), the definition of the variables (b) and the compatibility 'paths' (c).

Five compatibility conditions are formulated for bars AE, BE, CE, BD, and CD. The definition of the state variables is given in Fig. 11a–b.

Consider the structure in the position where nodes A, B, and C coalesce in the origin of the coordinate system, and node D is at $(0,0,1)$. The structure may leave this position by moving node E, which corresponds to a single parameter motion, e.g., a compatibility path. However, if node E remains in place, node D can move on the surface of a sphere with unit radius. This motion can be described by two parameters, thus it corresponds to a compatibility surface, which is a plane in this case. In the neighbourhood of the point in question three variables, $\phi_1$, $\phi_4$, and $\phi_5$ are sufficient (Fig. 11c).

## 8. Conclusions

This paper has shown that a number of variables ($n$) are in general required to uniquely define the compatible positions of SDOF mechanisms. The variables have to satisfy $n-1$ compatibility equations. Based on this, we have introduced an energy function to classify the compatible positions. The classification also depends on which element is regarded actuated. Classes of compatibility points can be paralleled to those of equilibrium positions of elastic structures under a single-parameter loading known in the literature, in spite of that in the latter case all stationary points refer to equilibrium positions, and the order of the energy function at the singular points is different.

## Acknowledgments

The authors acknowledge the financial support of The European Science Exchange Programme by The Royal Society. The work of the first author was also supported by University Graduate Scholarship at St Edmund Hall, University of Oxford and the Hungarian Grant OTKA D45978. The second author thanks the support of the Hungarian Grant FKFP 0308/2000 and OTKA T031931.

## References

Arnol'd, V.I., 1972. Normal forms for functions near degenerate critical points, the Weyl groups of $A_k$, $D_k$, and $E_k$, and Lagrangian singularities. Funkcional Anal. i Priložen 6, 3–25, Functional Anal. Appl. 6 (1972) 254–272.

Domokos, G., 1991. An elastic model with continuous spectrum. International Series of Numerical Mathematics 97, 99–103.

Gáspár, Zs., 1999. Stability of elastic structures with the aid of catastrophe theory. In: Kollár, K. (Ed.), Structural Stability in Engineering Practice. E&FN Spon, London, Chapter 4.

Gáspár, Zs., 2003. Mechanical models for the subclasses of catastrophes. In: Phenomenological and Mathematical Modelling in Structural Instabilities, CISM Courses and Lectures, Udine, Italy, 20–24 October 2003, in press.

Gáspár, Zs., Mladenov, K.A., 1995. Post-critical behaviour of a column loaded by a polar force. In: Iványi, M., Verőci, B. (Eds.), Preliminary Report of Colloids on Stability of Steel Structures, Budapest, II/275–281.

Gáspár, Zs., Németh, R., 2002. Models for visualisation of special losses of stability (in Hungarian), Scientific Publications of the Department of Structural Engineering, Faculty of Civil Engineering, Budapest University of Technology and Economics, pp. 81–92.

Gáspár, Zs., Domokos, G., Szeberényi, I., 1997. A parallel algorithm for the global computation of elastic bar structures. Computer Assisted Mechanics and Engineering Sciences 4, 55–68.

Géradin, M., 2001. Finite element simulation of deployable structures. In: Deployable Structures, CISM Courses and Lectures, No. 412, Udine, Italy, 5–9 July 1999, Springer, Wien, New York, 2001, pp. 239–360.

Lengyel, A., 2002. Analogy between equilibrium of structures and compatibility of mechanisms, PhD dissertation, University of Oxford, UK.

Lengyel, A., You, Z., 2003. Analogy between bifurcations in stability of structures and kinematics of mechanisms. Mechanics Based Design of Structures and Machines 31 (4), 491–507.

Lengyel, A., You, Z., 2004. Bifurcations of SDOF mechanisms using catastrophe theory. International Journal of Solids and Structures 41 (2), 559–568.

Litvin, F.L., 1980. Application of theorem of implicit function system existence for analysis and synthesis of linkages. Mechanism and Machine Theory 15, 115–125.

Poston, T., Stewart, I., 1978. Catastrophe Theory and its Applications. Pitman, London.

Tarnai, T., 1990. Kinematically indeterminate structures and structural topology (in Hungarian), DSc thesis, Hungarian Academy of Sciences, Budapest, Hungary.

Tarnai, T., 1999. Rigidity and kinematic bifurcation of structures. 40th Anniversary Congress of the International Association for Shell and Spatial Structures 1, B 2.81–B 2.90, CEDEX.

Thompson, J.M.T., Hunt, G.W., 1984. Elastic Instability Phenomena. Wiley, Chichester.